Automatic Aircraft Landing Over Parabolic Trajectory Using Precise GPS Measurements

S Agarwal
Cranfield University
College Road, Bedfordshire
United Kingdom, MK43 0AL

saurav.agarwal@cranfield.ac.uk

H B Hablani
Indian Institute of Technology Bombay
Powai, Mumbai
India, 400076

hbhablani@aero.iitb.ac.in

ABSTRACT

Global Positioning System (GPS) based aircraft landing is a methodology still not in use today despite the widespread use of GPS. This is primarily because a standard single frequency Global Positioning System (GPS) receiver provides a positioning accuracy of approximately 4-20 m which is not acceptable by aviation standards for precision landings. The accuracy of GPS can be further enhanced with dual frequency receivers which are able to provide accuracy around 1-12 m. However, these errors are still quite large when it comes to critical safety of life applications. Differential GPS (D-GPS) allows for precise positioning using information from reference stations on the ground along with satellite signals. Carrier phase tracking is one such D-GPS approach which allows range determination with centimeter level accuracy. However, carrier phase measurements require estimation of unknown fixed integer ambiguities before the receiver can start determining its position. Using single difference smoothed pseudorange measurements the integer ambiguities can be estimated with reasonable accuracy. This methodology brings the position error down to centimeter level which can meet the Federal Aviation Authority (FAA) regulations for Category-III (CAT-III) precision approaches. This paper examines an aircraft automatic landing using single differenced smoothed pseudorange measurements as the primary navigation source for an aircraft. The use of a parabolic descent trajectory is explored. Simulations demonstrate positioning with centimeter level accuracy using smoothed pseudorange measurements which enable a fully automatic landing. The accuracy is found to be dependent on the autopilot errors rather than the positioning system errors.

General Terms

Algorithm, Measurement, Performance, Reliability

Keywords

Global Positioning System, Dual frequency GPS, Pseudorange, Carrier Phase, Code Phase, Integer Ambiguity

1. INTRODUCTION

Developing countries which are looking to expand their regional aircraft operations can do so with minimal investment in expensive ground based signaling systems such as Instrument Landing System (ILS) by relying on satellite navigation. However, commercial satellite positioning (C/A code) does not offer the precision required for safety critical applications. D-GPS promises CAT-III accuracy using existing GPS receiver along with ground based reference stations using a methodology known as carrier phase tracking. However, carrier phase measurements are biased by unknown fixed integer numbers of cycles referred to as integer ambiguities. These values must be resolved to take full advantage of the carrier phase measurements. This is referred to as the integer ambiguity resolution problem.

In this paper, first dual frequency GPS measurements are described and the simulation results of a standalone Dual-Frequency GPS receiver during flight are presented. An algorithm is presented for integer ambiguity resolution [7] that uses single difference smoothed pseudorange measurements. This method has an advantage that it requires minimal computation compared to the conventional algorithms such as the search methods and the motion-based algorithms. It enables the determination of integer ambiguities which allow the use of phase measurements for accurate positioning of the aircraft. The use of two additional ground based GPS signal sources called integrity beacons [1] placed on the approach path to the airport is also investigated. The paper goes on to explore the design of a parabolic descent trajectory. Simulation results of a precision automatic landing over a parabolic trajectory using a longitudinal autopilot for a Boeing 747 are then presented.

2. DUAL FREQUENCY RECIEVER EMULATION

For the determination of its position on earth, the GPS receiver compares the time when the signal was sent by the satellite with the time the signal was received. From this time difference the distance between receiver and satellite can be calculated. If data from other satellites are taken into account, the present position can be calculated by trilateration. By means of four or more satellites, an absolute position in a three dimensional space can be determined along with the user clock bias.

The user can estimate the pseudo range to a satellite 'i' using the following equation [2]:

$$\rho_i = c(t_{Au} - t_{Ts}) \quad (1)$$

Where:

$$t_{Au} = t_A + b_u + v \quad (2)$$

$$t_A = t_T + \frac{D}{c} + T + I \quad (3)$$

$$t_{Ts} = t_T + B \quad (4)$$

ρ_i : Measured pseudorange to the ith satellite

t_{Au} : Measured time of arrival of signal at user

t_{Ts} : Value of time of transmission in message

t_A : True time of arrival at user

t_T: True time of transmission from satellite

T: Tropospheric delay [3]

I: Ionospheric delay [4]

D: Geometric range from user to satellite

B : Satellite clock error

b_u : User clock bias

v: Receiver measurement noise

c: Speed of light

It can be seen from the above equations, the user needs to apply certain corrections to the measured pseudo range for the satellite clock bias which are transmitted in the GPS message. By using iono-free pseudo range measurements with a dual frequency receiver it is also possible to eliminate the iono-delay [6]. This is possible because the iono-delay is inversely proportional the frequency.

$$\rho_{if} = 2.546\rho_{L1} - 1.546\rho_{L2} \qquad (5)$$

ρ_{L1} : Pseudorange measurement using L1 carrier signal

ρ_{L2} : Pseudorange measurement using L1 carrier signal

$$\rho_{if} = \rho_{Ti} + c(\delta_i - \delta_R) + T + \upsilon \qquad (6)$$

Where ρ_{Ti} is the real range from the ith satellite to the receiver. The pseudorange contains two primary sources of error. The two error sources are: (a) errors in the inaccurate receiver clock (δ_R), called the receiver clock offset; and (b) errors in the inaccurate satellite receiving signal (δ_i). Note that an important property of δ_R is that it is the same for all satellite signals and pseudoranges since it is a property of the receiver. The tropospheric delay and noise are neglected as they cannot be determined by the user. Therefore, Eqn (6) becomes:

$$\rho_{if} \cong \rho_{Ti} + c(\delta_i - \delta_R) \qquad (7)$$

$$\rho_{Ti} = \sqrt{(X - X_i)^2 + (Y - Y_i)^2 + (Z - Z_i)^2} \qquad (9)$$

The satellite's position is denoted as (X_i, Y_i, Z_i) and the receiver's position as (X, Y, Z). The satellite position is calculated by the receiver from the ephemerides in the navigation message. The right side of Eq. (7) contains the four unknowns of X, Y, Z, and δ_R. Hence, to solve for the four unknowns; a minimum of four satellites is required to yield four equations. Since Eqn. (7) is nonlinear, typically this is done using the multidimensional Newton–Raphson method and a reasonable guess of the initial receiver position [5]. The initial guess is at (X_0, Y_0, Z_0).

$$X = X_0 + \Delta X, Y = Y_0 + \Delta Y, Z = Z_0 + \Delta Z \qquad (8)$$

Where X, Y, Z is the true ECEF solution and ΔX, ΔY and ΔZ is the difference between the true solution and the initial guess. The initial guess at the receiver ECEF coordinates yields an initial guess for the true range. To correct the initial guess, ΔX, ΔY, ΔZ need to be determined in order to update X_0, Y_0, and Z_0. This is done by a linear (first-order Taylor) expansion of ρ_{if} in the three spatial coordinates.

$$\rho_{if} - \rho_{Ti} - c\delta_i = \Delta X \frac{\partial \rho_i}{\partial X}|_{X_0,Y_0,Z_0} + \Delta Y \frac{\partial \rho_i}{\partial Y}|_{X_0,Y_0,Z_0} + \Delta Z \frac{\partial \rho_i}{\partial Z}|_{X_0,Y_0,Z_0} - c\delta_R$$

$$(9)$$

The solution ΔX, ΔY, ΔZ and δ_R can be found using a minimum of four equations. Defining,

$$l = \begin{bmatrix} \rho_1 & -c\delta_1 & \rho_{T1} \\ \rho_2 & -c\delta_2 & \rho_{T2} \\ \rho_3 & -c\delta_3 & \rho_{T3} \\ \rho_4 & -c\delta_4 & \rho_{T4} \end{bmatrix}$$

$$A = \begin{bmatrix} \Delta X \frac{\partial \rho_1}{\partial X}|_{X_0,Y_0,Z_0} & \Delta Y \frac{\partial \rho_1}{\partial Y}|_{X_0,Y_0,Z_0} & \Delta Z \frac{\partial \rho_1}{\partial Z}|_{X_0,Y_0,Z_0} & 1 \\ \Delta X \frac{\partial \rho_2}{\partial X}|_{X_0,Y_0,Z_0} & \Delta Y \frac{\partial \rho_2}{\partial Y}|_{X_0,Y_0,Z_0} & \Delta Z \frac{\partial \rho_2}{\partial Z}|_{X_0,Y_0,Z_0} & 1 \\ \Delta X \frac{\partial \rho_3}{\partial X}|_{X_0,Y_0,Z_0} & \Delta Y \frac{\partial \rho_3}{\partial Y}|_{X_0,Y_0,Z_0} & \Delta Z \frac{\partial \rho_3}{\partial Z}|_{X_0,Y_0,Z_0} & 1 \\ \Delta X \frac{\partial \rho_4}{\partial X}|_{X_0,Y_0,Z_0} & \Delta Y \frac{\partial \rho_4}{\partial Y}|_{X_0,Y_0,Z_0} & \Delta Z \frac{\partial \rho_4}{\partial Z}|_{X_0,Y_0,Z_0} & 1 \end{bmatrix}$$

$$\delta x = \begin{bmatrix} \Delta X \\ \Delta Y \\ \Delta Z \\ c\delta_R \end{bmatrix}$$

$$l = A\delta x \qquad (10)$$

Using these Eqn. (10), the solution is $\delta x = A^{-1}l$. After solving for ΔX, ΔY, ΔZ and δ_R the corrected coordinates are updated to yield X, Y, and Z. This solution is, of course, an approximation so an iterative approach is required whereupon the most recent solution becomes the initial guess and the process above is repeated until the desired accuracy is obtained. The receiver needs to take care of the fact that any random combination of 4 satellites from the visible satellites cannot be used. The receiver must check for optimal geometry by calculating the Geometric Dilution of Precision (GDOP) value for all possible combinations and selecting the combination that offers the lowest possible GDOP.

$$GDOP = \sqrt{Q_{11}^2 + Q_{22}^2 + Q_{33}^2 + Q_{44}^2} \qquad (11)$$

Where,

$$Q = (A^T A)^{-1}$$

2.1 Simulation Results

A point to point flight from Delhi airport to Mumbai Airport at 10,000 m altitude was simulated. There are no atmospheric disturbances to the aircraft and it is assumed to be flying at constant velocity. The error in position is plotted in Figure 1. The error in position (magnitude of distance between true position and actual position) is between 0-8 m. Figure 2 shows the error in velocity estimation by GPS.
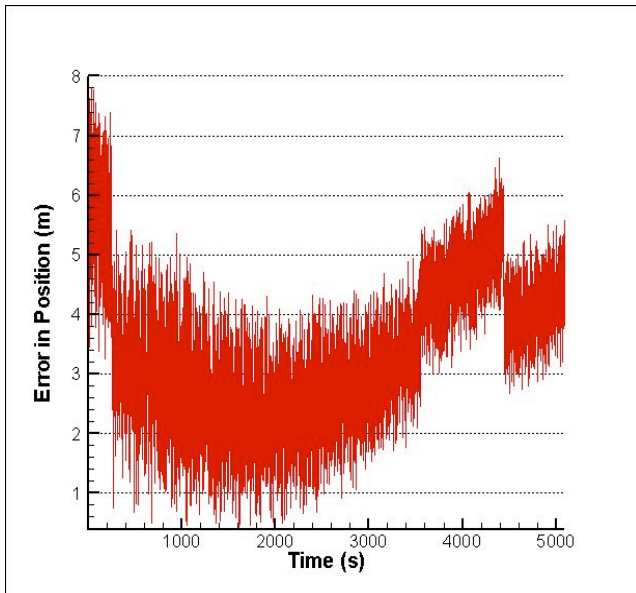
Figure 1: Error in position (m)
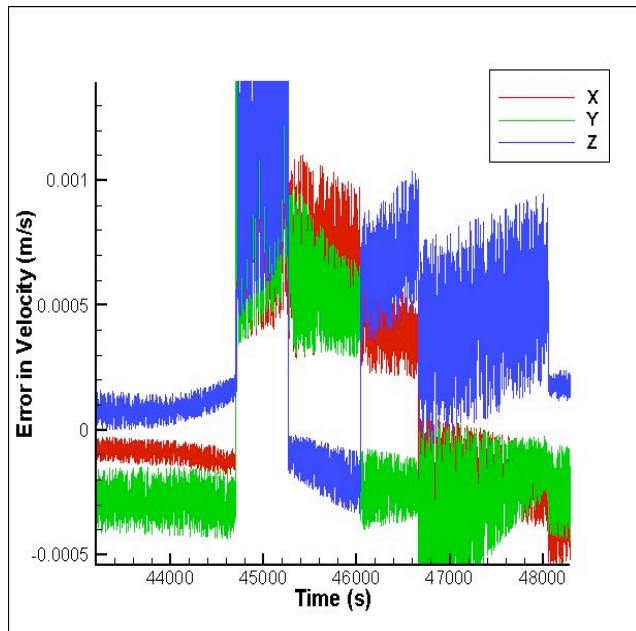
Figure 2: Error in velocity measurement (ECEF Frame)
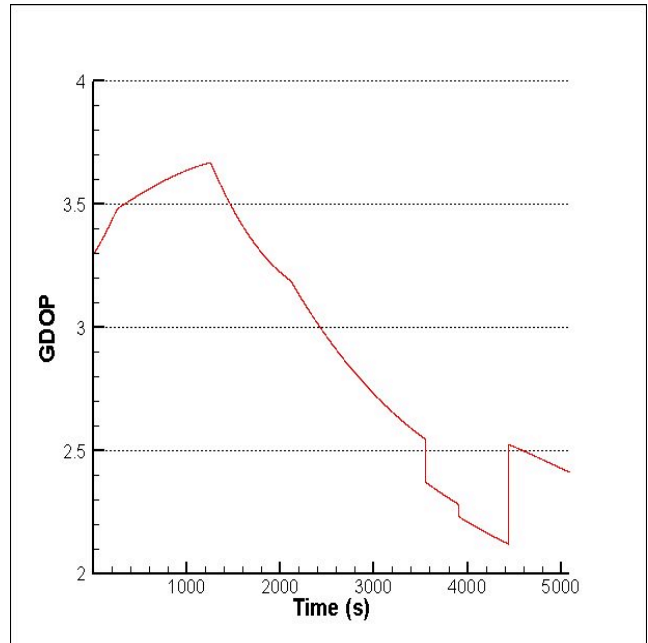
Figure 3: Variation of GDOP during flight
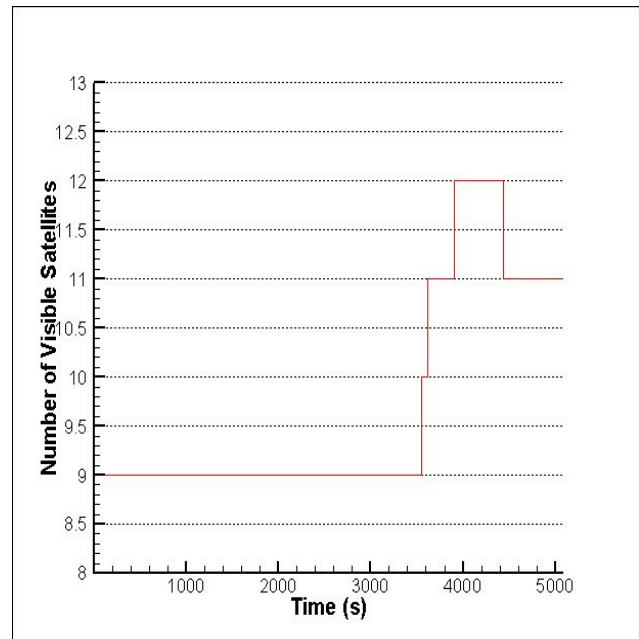
Figure 4: Satellite visibility during flight

Figure 3 shows the variation of the GDOP during flight which can related to the positioning accuracy. As the GDOP is falling the accuracy increases. Figure 4 depicts the number of satellites visible during the flight. It can be seen that when a new satellite is introduced there is a marked reduction in the GDOP due to the availability of better satellite geometry. When the number of satellites reduces the GDOP increases due to poor geometry.

3. CARRIER PHASE TRACKING

According to [6] the carrier phase can be measured with a precision of 0.01-0.05 cycle (2mm-1cm). Precise positioning which is interpreted as centimeter-level positioning requires carrier phase measurements. The carrier phase measured at the user 'u' for the satellite 'k' is:

$$\phi_u^k = r_u^k - I_u^k + T_u^k + \lambda N_u^k + \tau_u^k + \varepsilon_{\phi,u}^k \qquad (12)$$

Where,

r_u^k : Geometric range from user to satellite

I_u^k : Advance in phase due to ionosphere

T_u^k : Delay in phase due to troposphere

N_u^k : Integer ambiguity

λ : Carrier wavelength

τ_u^k : Clock bias between user and satellite

$\varepsilon_{\phi,u}^k$: Measurement noise

Similarly for a reference receiver 'r':

$$\phi_r^k = r_r^k - I_r^k + T_r^k + \lambda N_r^k + \tau_r^k + \varepsilon_{\phi,r}^k \qquad (13)$$

Subtracting Eqn. (13) from (12):

$$\phi_{ur}^k = r_{ur}^k - I_{ur}^k + T_{ur}^k + \lambda N_{ur}^k + \tau_{ur} + \varepsilon_{\phi,ur}^k \qquad (14)$$

Eqn. (14) gives what is called the single difference phase measurement. For short baselines i.e. when the user and reference are close it can be assumed that ionospheric and tropospheric delays are nearly the same and hence neglecting those terms:

$$\phi_{ur}^k \cong r_{ur}^k + \lambda N_{ur}^k + \tau_{ur} + \varepsilon_{\phi,ur}^k \qquad (15)$$

Thus, if the fixed integer ambiguities can be estimated, the relative vector from the reference to the user can be determined.

3.1 Pseudorange Smoothing[7]

The single difference code phase measurements can be calculated similar to the single difference carrier phase as:

$$\rho_{ur}^k \cong r_{ur}^k + \tau_{ur} + \varepsilon_{\phi,ur}^k \qquad (16)$$

Subtracting Eqn. (16) from Eqn. (15) the smoothed pseudorange measurement is obtained [6]:

$$\phi_{ur}^k - \rho_{ur}^k \cong \lambda N_{ur}^k + \varepsilon_{\phi,ur}^k \qquad (17)$$

Thus, from Eqn. (17) it can be seen that the value of the integer ambiguity can be easily estimated at a single epoch:

$$\hat{N} = round[\lambda^{-1}(\phi_{ur}^k - \rho_{ur}^k)] \qquad (18)$$

λ: Carrier signal wavelength

These measurements are however noisy, therefore to eliminate the measurement noise, the values of the integer ambiguities over multiple epochs are averaged to obtain the final estimate. Figure 5 shows the simulation results of integer ambiguity estimation at 100 epochs. The rounded off values are shown by the circles.

The standard deviation (σ) of error in integer estimation for 100 epochs is 2.63 cycles. The accuracy increases as the number of sampled points increases but this slows down the process of carrier phase tracking as the aircraft must wait longer before it can switch to CDGPS mode.
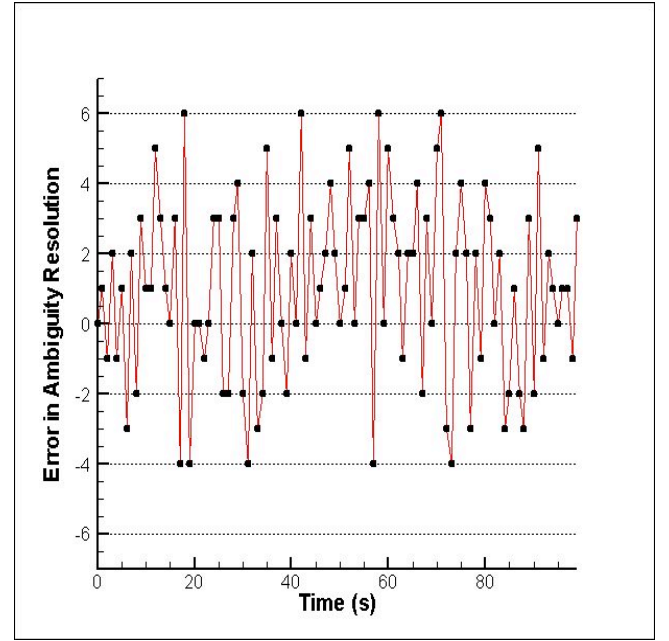
Figure 5: Error in ambiguity resolution for 100 epochs

4. LANDING USING INTEGRITY BEACONS [1]

A landing approach using carrier phase tracking was simulated to test the accuracy of the above mentioned method. The aircraft is assumed to equipped with a perfect INS to compare the results of pseudorange smoothing to the truth model. The airport is equipped with a precisely surveyed reference GPS receiver broadcasting its carrier and code measurements as well two integrity beacons placed approximately 16 km away from the airport on either side of the approach path. These integrity beacons provide the aircraft extra sources of measurements as well redundancy in case the user is unable to track the requisite number of satellites due to bad atmospheric conditions or Selective Availability. As the aircraft flies over these integrity beacons it starts collecting the smoothed pseudo range measurements as described in Eqn. (17). Such a maneuver is called a bubble pass. After collecting measurements over multiple epochs, the user averages the values and obtains the integer ambiguities according to Eqn. (18). Post resolution of the fixed

integer ambiguities, the user plugs them back into Eqn. (15). At any epoch 't' if there are 'n' satellites visible then there are 'n+2' (due to the two integrity beacons) such equations. An approximation is made that for short baselines that the line of sight vectors from the reference and user to a satellite are nearly the same.

Thus for satellite 'k':

$$\phi_{ur}^k \cong -\vec{s}_{ur}^k \cdot \vec{x} + \lambda N_{ur}^k + \tau_{ur} + \varepsilon_{\phi,ur}^k \qquad (19)$$

$\vec{x}$: Relative position of the user w.r.t the reference station

$\vec{s}_{ur}^k$: Line of sight vector to satellite

Similarly for the integrity beacon 'j':

$$\varphi_{ur}^k = \left| \vec{p}_j - \vec{x} \right| - \left| \vec{p}_j \right| + \lambda N_{ur}^j + \tau_{ur} + \varepsilon_{\phi,ur}^k \qquad (20)$$

p_j : Relative vector from reference station to integrity beacon j

Given an approximate trajectory $\hat{\vec{x}}$, obtained from code based measurements, the above equations can be expressed in terms of the deviation from the approximate trajectory $\delta x = \vec{x} - \hat{\vec{x}}$,

$$\delta\phi_{ur}^k = \phi_{ur}^k + \vec{s}_{ur}^k \cdot \vec{x} = -\vec{s}_{ur}^k \cdot \delta\vec{x} + \lambda N_{ur}^k + \tau_{ur} + \varepsilon_{\phi,ur}^k \qquad (21)$$

$$\delta\varphi_{ur}^j = \varphi_{ur}^j - \left| \vec{p}_j - \vec{x} \right| + \left| \vec{p}_j \right| = -\vec{e}_{ur}^j \cdot \delta\vec{x} + \lambda N_{ur}^j + \tau_{ur} + \varepsilon_{\phi,ur}^j$$

$$(22)$$

Where,

$\vec{e}_{ur}^j$: Line of sight vector from integrity beacon j to user

Therefore, the measurements at a single epoch are stacked as:

$$\delta\phi = \begin{bmatrix} \delta\phi_{ur}^1 \\ . \\ . \\ . \\ \delta\phi_{ur}^n \\ \delta\varphi_{ur}^1 \\ \delta\varphi_{ur}^2 \end{bmatrix} \quad N = \begin{bmatrix} N_{ur}^1 \\ . \\ . \\ . \\ N_{ur}^n \\ N_{ur}^{IB2} \\ N_{ur}^{IB1} \end{bmatrix} \quad \hat{S} = \begin{bmatrix} -\vec{s}_{ur}^{1T} & 1 \\ . & . \\ . & . \\ . & . \\ -\vec{s}_{ur}^{nT} & 1 \\ -\vec{e}_{ur}^{1T} & 1 \\ -\vec{e}_{ur}^{2T} & 1 \end{bmatrix} \quad \delta x^* = \begin{bmatrix} \delta x \\ \tau_{ur} \end{bmatrix}$$

$$(\delta\phi - N) = \hat{S}\delta x^* \qquad (23)$$

Using least squares estimation, Eqn. (23) can be solved to update the relative vector till the solution converges to a desired value.

4.1 Simulation Results

A landing was simulating assuming a perfect Inertial Navigation System on board the aircraft to determine the positioning accuracy of carrier phase smoothing. Figure 6 shows the error in position as the aircraft approaches Delhi airport. For the first 120 s the aircraft is collecting the phase measurements for each epoch and relying on dual frequency GPS. After collecting this data, the navigation system calculates the integer ambiguities using the method described in section 3. Post t = 120 s, the aircraft uses carrier phase tracking (parallel to ILS where aircraft tracks glide slope upon reaching the outer marker). Figure 6 shows that as the aircraft switches from dual frequency GPS to carrier phase tracking at t = 120s, the error in position drops drastically close to 1.4 m. As time progresses, for shorter baselines the error is gradually reducing. Figure 7 shows the error in position during carrier phase differential GPS (CDGPS) mode.
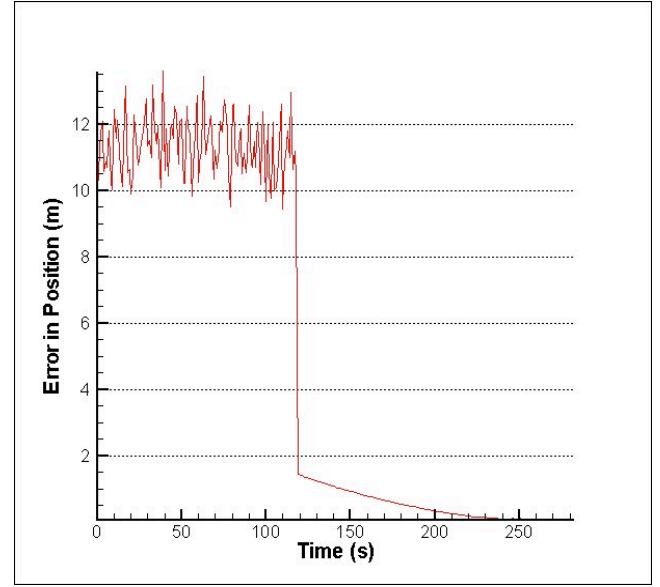
Figure 6: Error in position during airport approach (m)
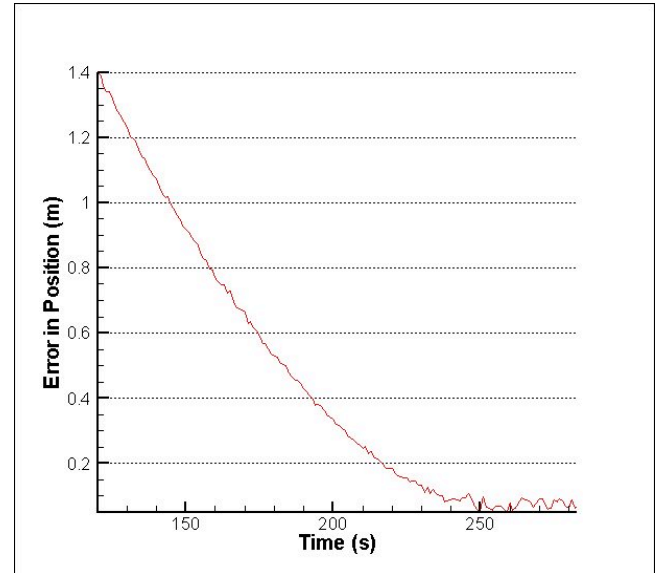
Figure 7: Error in position during CDGPS mode

5. MEETING FAA REGULATIONS

The FAA navigation accuracy requirements for precision approaches using ILS are shown in Table I.

Table 1. FAA requirements for precision approach

Category	Visibility	Decision Height	Accuracy Req. 95% limits
CAT I	800 m	60 m	Horizontal 16.5 m Vertical 3.4 m
CAT II	360 m	30 m	Horizontal 6.5 m Vertical 1.6 m
CAT IIIa	> 210 m	< 30 m	Horizontal 4.1 m Vertical 0.5 m
CAT IIIb	45-210 m	< 15 m	
CAT IIIc	< 45 m	0	

As seen from the Table I, for matching CAT-IIIa requirements for landing aircrafts cannot rely on traditional GPS positioning. Carrier phase tracking using integrity beacons on the ground is easily able to match CAT-IIIa requirements. Table II shows the navigation accuracy using carrier phase positioning. The error falls well below the range defined by the FAA.

Table 2. Navigation accuracy of CDGPS

Dimension	Mean Error	Standard Deviation (σ)
Horizontal	0.07 m	0.059 m
Vertical	0.25 m	0.31 m

6. AUTOMATIC LANDING SIMULATION

An automatic landing was simulated for a Boeing 747, a longitudinal autopilot was simulated since GPS measurements tend to be more erroneous in the vertical as seen from Table 2. We explore the use of a parabolic descent path. Such a trajectory can in the future be used for a Continuous Descent Approach which allows the aircraft to descend from high altitudes to the runway in a smooth manner. This approach has been shown to reduce fuel consumption and enables significant noise reduction which is a concern in cases where airports are located near populated areas[8]. According to tests by Boeing and the FAA, CDA at a single airport can save millions of liters of fuel, and reduce atmospheric carbon dioxide emissions significantly. Figure 8 shows the system architecture of a GPS based landing system.
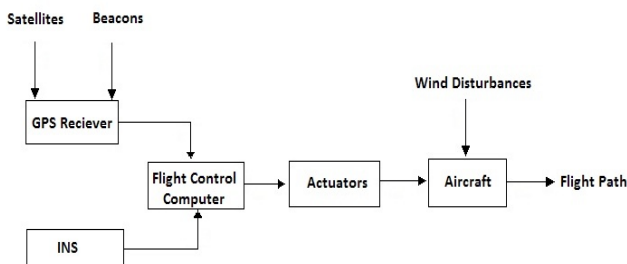
Figure 8: System Architecture

6.1 Approach Trajectory Design

A traditional trajectory for landing makes use of a linear descent followed by thrust increase to level out. This method is followed recursively till the aircraft intercepts the ILS signal. The ILS signal usually has a 2-3 degree glideslope. A parabolic continuous descent trajectory was examined for the landing simulation. The use of GPS based navigation allow us to design such a trajectory which would traditionally not be possible with conventional ILS systems which only allow straight line descents. Such a trajectory is considerably easy for an autopilot to follow compared to a human pilot and allows for minimal fuel usage during the procedure. Approximately 50 m above the runway the aircraft switches over to an exponential trajectory for the flare phase which allows for a smooth touchdown within load limits of the aircraft. Figure 9 shows the approach trajectory used for the simulations.
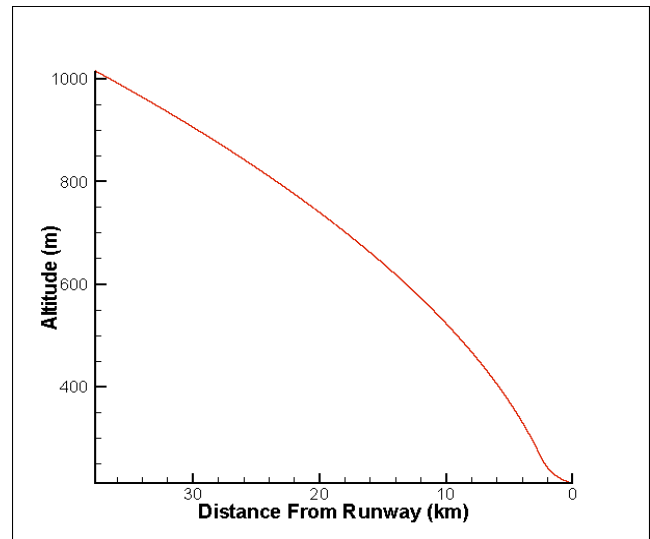
Figure 9: Parabolic landing trajectory

6.2 Landing Autopilot Design

Classical control design methods were used to arrive at the landing autopilot controller. The longitudinal mode of the Boeing 747 in landing configuration was examined. The autopilot is designed to minimize the vertical deviation 'd' from the designed trajectory while maintaining the airspeed. The automatic control of the trajectory requires the simultaneous control of thrust and pitch attitude because otherwise, using only the elevator to gain altitude would result in a loss of airspeed.
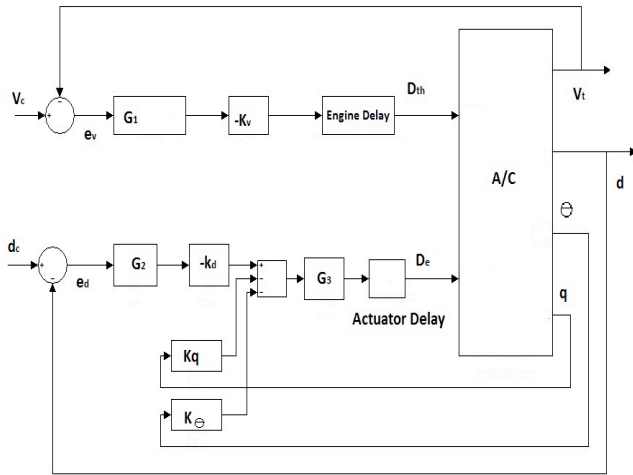
Figure 10: Landing autopilot design

Figure 10 shows the design of the autopilot where,

V_c: Control input for velocity

d_c: Control input for vertical deviation

$G_{1/2/3}$: Controllers

k_q: Pitch rate gain

k_Θ: Pitch attitude gain

D_{th}: Throttle Input

D_e: Elevator deflection

A/C: Aircraft Dynamics

V_t: Aircraft Velocity

d: Vertical deviation from glideslope

6.3 Simulation Results

A Boeing 747 in landing configuration is assumed to be approaching the runway. The runway is at an altitude of 216 m. Wind disturbances have been accounted for with a heavy 15 m/s head wind with a random variation modeled as Gaussian noise, similarly there is an updraft of 5 m/s with random variation modeled as Gaussian noise. Sensor errors have been modeled as Gaussian white noise disturbances scaled appropriately. Figure 11

shows the simulation results for trajectory following. Prior to t = 100 seconds the aircraft is relying on standard dual frequency GPS measurements. After t = 100 seconds the aircraft switches to carrier phase positioning using smoothed pseudorange measurements.

Figure 12 shows the vertical deviation from the glideslope. It can be seen that there is a considerable error in the aircraft trajectory from the design trajectory prior to the switch. The error falls rapidly when the aircraft switches to differential GPS. The error rises as the trajectory becomes more vertical near the end which can be ascribed to the slow response of a heavy aircraft. Another reason for the error is the wind disturbance. The mean error is 0.85 m in the vertical ('d'). The standard deviation (σ) is 1.72 m.
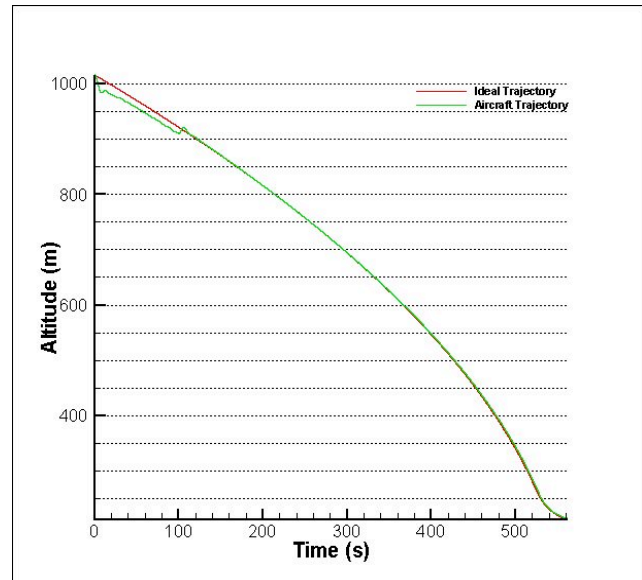
Figure 11: Aircraft trajectory vs. ideal trajectory
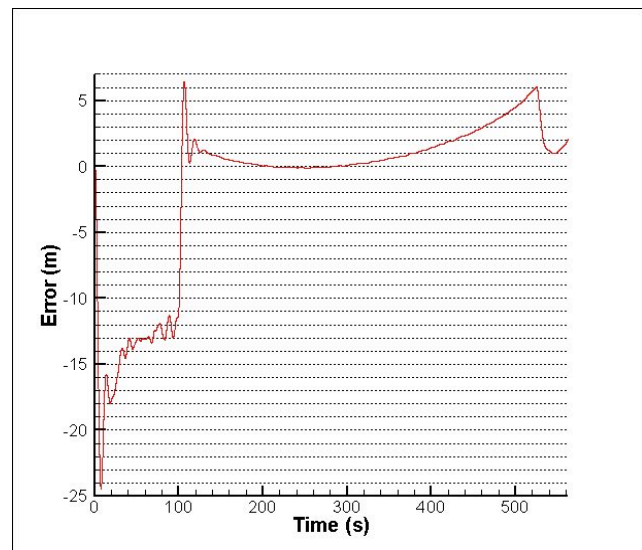
Figure 12: Vertical deviation from glideslope
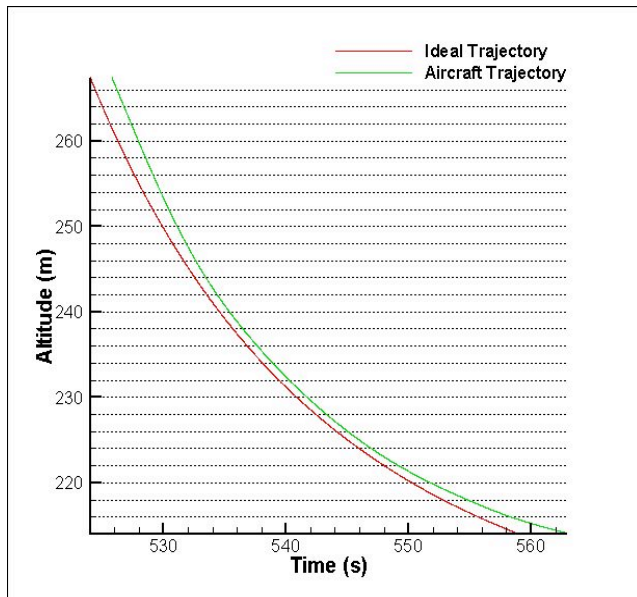
Figure 13: Flare Phase

Figure 13 shows the flare phase of the landing. The aircraft is flying above the designed trajectory which can mainly be attributed to the fact that the wind disturbances were high.

7. Conclusions

Simulations show that a dual frequency receiver is accurate enough to provide reliable in-flight navigation, however it cannot be used for precision landing as the errors are quite large. Precise positioning using carrier phase tracking using smoothed pseudorange measurements for integer ambiguity resolution shows promising results for CAT-III approaches. One drawback is that the integer ambiguity resolution is not real time and requires that the user collect data from multiple epochs before a reliable estimate of the ambiguity can be made. This can be removed in the future with the advent of the additional L5 GPS frequency. [6] Describes a method using L1, L2 and L5 frequencies for real time estimation of the ambiguities with increased accuracy ($\sigma = 0.3$ cycles). Simulations of automatic landing using smoothed pseudorange measurements show that performance of landing system are dominated by the autopilot error and not the system accuracy. The autopilot accuracy can be increased with the use of more sophisticated control system designs such as Linear Quadratic Gaussian Controllers. The use of a continuous descent approach was explored as one of the future applications for satellite based landing systems. Such a system can even allow for curved trajectories allowing incoming aircrafts to approach from multiple directs before converging. This would be make the air traffic flow smoother and more efficient as it would remove the restriction of aligning aircrafts on a straight approach path from far away.

8. REFERENCES

[1] Cohen, C.E., Pervan, B.S., Cobb, H.S., "Precision Landing of Aircraft Using Integrity Beacons", in Parkinson, B.W and Spilker Jr. J.J., Global Positioning System: Theory and Applications Volume II, Vol. 163 Progress In Aeronautics and Astronautics, AIAA, 1996, pp. 427-459

[2] Parkinson, B.W, "GPS Error Analysis", in Parkinson, B.W and Spilker Jr. J.J., Global Positioning System: Theory and Applications Volume I, Vol. 163 Progress In Aeronautics and Astronautics, AIAA, 1996, pp. 469-483

[3] Hopsfield, H.S., "Tropospheric Effect on Electromagnetically Measured Range: Prediction from Surface Weather Data", Applied Physics Laboratory, Johns Hopkins University, Baltimore, MD, July 1970

[4] Klobuchar, J.A., "A First-Order, Worldwide, Ionospheric Time Delay Algorithm", AFCRL-TR-75-0502, AD A018862, available from the Defense Technical Information Center, Cameron Station, Alexandria, VA 22304

[5] Axelrad P., Brown, R.G., "GPS Navigation Algorithms", in Parkinson, B.W and Spilker Jr. J.J., Global Positioning System: Theory and Applications Volume I, Vol. 163 Progress In Aeronautics and Astronautics, AIAA, 1996, pp. 409-433

[6] Misra, P., and Enge, P., "GPS Signals, Measurements, and Performance", 2nd Ed., Ganga-Jamuna Press, 2006, pp. 233-280

[7] Lundberg, J.B., Yoon S.P., "An Integer Ambiguity Resolution Algorithm for Real Time GPS Attitude Determination", Applied Mathematics and Computation 129 (2002) 21-41, Elsevier

[8] Zou, F., "Real Time Trajectory Optimization and Air Traffic Control Simulation for Noise Abatement Procedures", M.S Thesis, Massachusetts Institute of Technology, 2004